Traffic 2007; **8:** 1404–1414
Blackwell Munksgaard

doi: 10.1111/j.1600-0854.2007.00619.x

Mucolipin-2 Localizes to the Arf6-Associated Pathway and Regulates Recycling of GPI-APs

Claudia Karacsonyi, Anitza San Miguel and Rosa Puertollano*

Laboratory of Cell Biology, National Heart, Lung, and Blood Institute, National Institutes of Health, Bethesda, MD 20892, USA
**Corresponding author: Rosa Puertollano, puertolr@mail.nih.gov*

In mammals, the mucolipin family includes three members mucolipin-1, mucolipin-2, and mucolipin-3 (MCOLN1–3). While mutations in MCOLN1 and MCOLN3 have been associated with mucolipidosis type IV and the *varitint-waddler* mouse phenotype, respectively, little is known about the function and cellular distribution of MCOLN2. Here we show that MCOLN2 traffics via the Arf6-associated pathway and colocalizes with major histocompatibility protein class I (MHCI) and glycosylphosphatidylinositol-anchored proteins (GPI-APs), such as CD59 in both vesicles and long tubular structures. Expression of a constitutive active Arf6 mutant, or activation of endogenous Arf6 by transfection with EFA6 or treatment with aluminum fluoride, caused accumulation of MCOLN2 in enlarged vacuoles that also contain MHCI and CD59. In addition, overexpression of MCOLN2 promoted efficient activation of Arf6 *in vivo,* thus suggesting that MCOLN2 may have a role in the traffic of cargo through the Arf6-associated pathway. In support of this we found that overexpression of a MCOLN2 inactive mutant decreases recycling of CD59 to the plasma membrane. Therefore, our results indicate that MCOLN2 localizes to the Arf6-regulated pathway and regulates sorting of GPI-APs.

Key words: Arf6, GPI, MCOLN2, MLIV, mucolipin, TRP

Received 13 February 2007, revised and accepted for publication 3 July 2007, uncorrected manuscript published online 5 July 2007, published online 29 July 2007

Mucolipins constitute a family of cation channels with homology to the transient receptor potential superfamily (1). In mammals, the mucolipin family includes three members named mucolipin-1, mucolipin-2, and mucolipin-3 (MCOLN1-3) that exhibit a common six-membrane-spanning topology. Homologs of mammalian mucolipins have also been described in *Drosophila* and *Caenorhabditis elegans*. MCOLN1 is the best-characterized member of the mucolipin family, as mutations in this protein have been linked to mucolipidosis type IV (MLIV), a recessive lysosomal storage disease characterized by severe neurological and ophthalmologic abnormalities. It has been suggested that mutations in the MCOLN1 channel cause defects in late-endosomal/lysosomal trafficking, resulting in the accumulation of enlarged vacuolar structures that contain phospholipids, mucopolysaccharides, and gangliosides (2–5). In agreement with this idea, loss-of-function mutations in cup-5, the *C. elegans* ortholog of MCOLN1, resulted in the formation of large endosome–lysosome hybrid organelles that contain both late-endosomal and lysosomal markers (6–8).

MCOLN3 might also play a role in different human pathologies, as mutations in this gene are responsible for the *varitint-waddler* mouse phenotype that is characterized by defects in pigmentation and hearing loss (9). MCOLN3 is located in hair cells and it could be implicated in hair-cell maturation and melanosomes trafficking. It is important to note that the phenotype of cup-5 cells can be rescued by transfection with either human MCOLN1 or MCOLN3, suggesting that the function of these two proteins may be redundant to some extent (8).

MCOLN2 is also encoded within the *varitint-waddler* allele and has been proposed as a candidate gene for neurosensory disorders (9). In addition, MCOLN2 is expressed in primary B-lymphocytes and is a target for Bruton's tyrosine kinase, suggesting a possible role of MCOLN2 in B-lymphocyte development (10). However, mutations in MCOLN2 have not yet been associated with any human pathology and the function and cellular distribution of the protein remains to be characterized.

One approach to gaining information about the function of a protein is to study its trafficking and cellular distribution. For example, consistent with its role in lysosomal biogenesis, MCOLN1 has specific sorting motifs that mediate interaction with clathrin adaptors and the subsequent delivery of MCOLN1 to lysosomes (our unpublished observations) (11,12). Clathrin adaptors recognize tyrosine or di-leucine-based motifs located in the cytosolic tail of cargo proteins and, together with clathrin, regulate sorting of these cargo proteins between the trans-Golgi network (TGN) and the endosomal–lysosomal pathway as well as endocytosis from the plasma membrane (13).

Proteins that do not contain tyrosine or di-leucine-based motifs are endocytosed from the plasma membrane by using clathrin-independent pathways. In HeLa cells, internalization of class I molecules of the major histocompatibility complex (MHCI), interleukin-2 receptor, β_1 integrin, and many glycosylphosphatidylinositol-anchored proteins (GPI-APs), such as CD59, occurs by a clathrin-independent pathway regulated by the small GTP-binding protein

ADP-ribosylation factor 6 (Arf6) (14–16). After internalization these proteins reach sorting endosomes that also contain cargo internalized by the clathrin-dependent endocytic pathway. From sorting endosomes, Arf6 cargo proteins can be sorted to recycling endosomes and recycled back to the plasma membrane or delivered to lysosomes for degradation. Recycling of Arf6 cargo proteins has been exhaustively characterized and is known to be mediated by long tubular structures that contains Arf6 and requires the activity of several proteins, including Arf6, Rab11, Rab22 (17), Eps15 homology domain-containing protein (18), PLD (19), and TRE17 (20). In contrast very little is known about the proteins or conditions that regulate sorting of Arf6 cargo to lysosomes.

In this study, we analyzed the distribution and function of human MCOLN2 in HeLa cells. We chose HeLa cells for two reasons: first, the clathrin-dependent and the clathrin-independent pathways have been exhaustively characterized in this cell type; and second, we were able to detect expression of endogenous MCOLN2 in HeLa cells by reverse transcription–polymerase chain reaction (RT–PCR). Our results reveal that MCOLN2 traffics through the Arf6-associated pathway, colocalizing with MHCI and CD59 in long tubular endosomes as well as in Arf6Q67L-induced enlarged vacuoles. Moreover, MCOLN2 promoted activation of Arf6 *in vivo*, while overexpression of a MCOLN2 dominant-negative mutant decreased the rate of CD59 recycling to the plasma membrane. These observations suggest that MCOLN2 participates in the regulation of cargo traffic through the Arf6-regulated pathway.

Results

MCOLN2 localizes to the plasma membrane, intracellular vesicles, and tubular structures

The complete ORF of MCOLN2 (accession no. AY083533) was isolated from a human placenta cDNA library and cloned into the pDs-Red-Monomer-N1vector to produce a chimera that expresses red fluorescent protein (RFP) at the C-terminus of MCOLN2 (MCOLN2-RFP). Expression of MCOLN2-RFP in HeLa cells shows that the protein is present at the plasma membrane as well as in intracellular vesicles and tubular structures (Figure 1A). This distribution is clearly different from that of MCOLN1-GFP, another member of the mucolipin family that localizes almost exclusively at late endosomes/lysosomes [Figure 1A and (11)]. In addition, overexpression of MCOLN1-GFP causes swelling of late endosomes/lysosomes while no enlarged structures were observed after overexpression of MCOLN2-RFP.

Colocalization experiments with several cellular markers revealed that MCOLN2-RFP is not significantly present at the TGN or early endosomes, as evidenced by the lack of colocalization of MCOLN2-RFP-positive vesicles with GGA3-VHSGAT-GFP or endogenous EEA1, respectively (data not shown and Figure 1B). In contrast, most of the intracellular vesicles containing MCOLN2-RFP were also stained with antibodies against CD63 (85.5% $\pm$ 0.8; $n = 213$), indicating that these structures correspond to late endosomes/lysosomes (Figure 1B). Interestingly, MCOLN2-RFP is also present at the plasma membrane and in long tubules that do not contain endosomal or lysosomal proteins. The long tubules observed in MCOLN2-RFP transfected cells are reminiscent of tubular endosomes in the Arf6-regulated recycling pathway (14,15). In agreement with this idea, we found that MCOLN2-RFP colocalizes with MHCI and CD59, two cargo proteins that traffic through the ARF6-associated pathway, at long tubular structures (Figure 2). Therefore, we concluded that MCOLN2-RFP is present at both the degradative and the Arf6-regulated pathways.

Expression of Arf6Q67L or Arf6 activation alters MCOLN2-RFP distribution

It has been previously described that expression of the constitutively active GTPase-deficient Arf6 mutant (Arf6Q67L) perturbs trafficking of those cargo proteins transported through the Arf6-associated pathway. Thus, MHCI, Tac, and CD59 accumulate in enlarged vacuolar structures in cells expressing Arf6Q67L, while clathrin-dependent cargo is absent from those structures (15,16,21). To confirm that MCOLN2-RFP traffics via the Arf6 pathway, we coexpressed Arf6Q67L-HA and MCOLN2-RFP in HeLa cells. As expected, MCOLN2-RFP was trapped in Arf6Q67L-associated vacuoles that also contain endogenous MHCI and CD59 (see arrows in Figure 3A and Figure S1). Accumulation of MCOLN2-RFP in enlarged vacuolar structures was also observed after transfection with EFA6, a GTP-exchange factor (GEF) that induces activation of endogenous Arf6 (22) (Figure 3B). In addition, it has been described that overexpressed Arf6 can generate protrusions at the cell surface in response to treatment with aluminum fluoride (AlF) (14). As seen in Figure 3C, MCOLN2-RFP and Arf6wt-HA localized to surface protrusions after incubation with AlF for 30 min. All together our results confirm that MCOLN2-RFP travels through the Arf6-regulated pathway.

It is important to note that, despite the clear accumulation of MCOLN2-RFP in Arf6-GTP positive structures, there is also a population of MCOLN2-RFP that remains at the perinuclear area and is not affected by Arf6 activation (see arrowheads in Figure 3 and Figure S1). This population colocalizes with late-endosomal/lysosomal markers such as CD63 and Lamp-1, corroborating that MCOLN2-RFP is also present at the degradative pathway (Figure 3D).

Expression of a constitutively active Rab5 mutant (Rab5Q79L-GFP), a GTP-binding protein implicated in endocytosis in the clathrin-dependent pathway, caused accumulation of MCOLN2-RFP in enlarged early endosomes

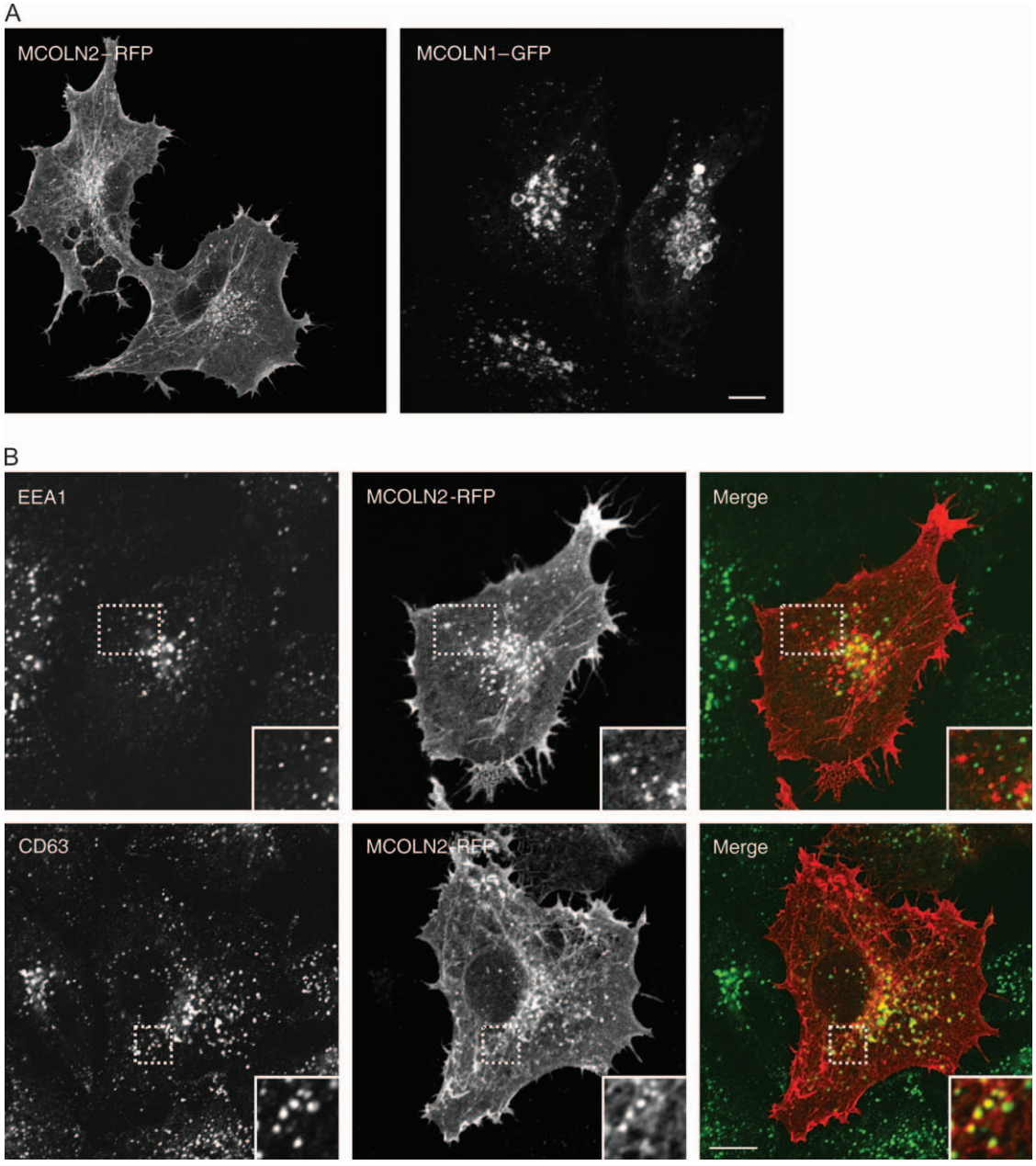

Figure 1: MCOLN2-RFP localizes to the plasma membrane, vesicles and long tubular structures. A) HeLa cells were grown on coverslips and transfected with MCOLN2-RFP or MCOLN1-GFP. Fifteen hours after transfection the cells were fixed and observed by confocal microscopy. Scale bar represents 10 μm. B) HeLa cells were transfected with MCOLN2-RFP, fixed, permeabilized, and immunostained with monoclonal antibodies to EEA1 or CD63 followed by Alexa-488-conjugated antibody to mouse IgG. The third picture of each row represents the merged confocal images; MCOLN2 is in red and yellow indicates colocalization. Inset show twofold magnifications of the indicated region. Scale bar represents 10 μm.

(Figure S2A). Interestingly, MCOLN2-RFP colocalized with CD59 (Figure S2B) and CD63 (Figure S2C) in Rab5Q79L-induced endosomes. These data are in agreement with previous reports indicating that non-clathrin-derived and clathrin-derived endosomes converge at early endosomes and that Tac, MHCI, and CD59 accumulate at Rab5Q79L-positive structures (16,21). On the basis of these observations we conclude that MCOLN2-RFP accesses to the degradative pathway through early endosomes.

MCOLN2-RFP induces Arf6 activation

To address the question of whether MCOLN2 is just a cargo protein that uses the Arf6 pathway to cycle between plasma membrane and intracellular compartments or

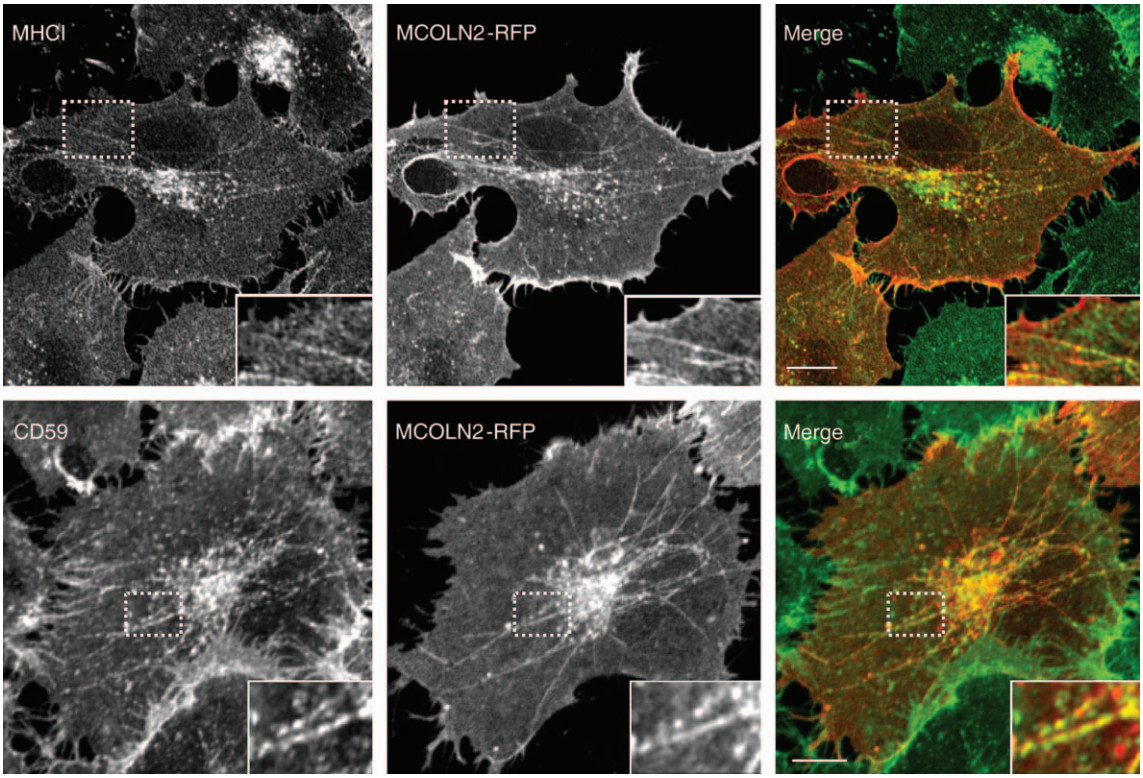

Figure 2: Colocalization of MCOLN2-RFP with MHCI and CD59 on tubular recycling endosomes. HeLa cells were transiently transfected with a construct encoding MCOLN2-RFP. After 15 h, the cells were fixed, permeabilized and incubated with an antibody against MHCI followed by incubation with Alexa-488-conjugated anti-mouse IgG. Alternatively, the cells were incubated with anti-CD59 monoclonal antibody for 30 min at 37°C, fixed, permeabilized, and incubated with Alexa-488-conjugated antibody to mouse IgG. MCOLN2 is in red. Insets show twofold magnifications of the indicated region. Scale bar represents 10 μm.

whether it has a specific function in this pathway, we decided to analyze overexpression of MCOLN2-RFP and correlate it to Arf6 activity. As shown in Figure 4A, Arf6wt-HA was mostly associated with the plasma membrane when expressed alone in HeLa cells. In contrast, coexpression of EFA6-FLAG allows efficient activation of Arf6wt that is now able to induce the formation of enlarged vacuoles, which are positive for both Arf6wt and EFA6 (see arrow in Figure 4B). Interestingly, coexpression of Arf6wt and MCOLN2-RFP also resulted in the formation of enlarged vesicles that resemble Arf6Q67L-induced vacuoles (Figure 4C), suggesting that MCOLN2-RFP might promote activation of Arf6.

To confirm this possibility we performed pull-down experiments using the Arf/GTP-binding domain of Golgi-localized ear-containing ARF-binding protein 1 (GGA1) fused to GST (GGA1GAT-GST). This assay has been used previously to quantify the amount of active Arf6 in a lysate (23–25). When expressed alone in HeLa cells, only a small percentage of Arf6wt was able to bind GGA1GAT-GST. However, when MCOLN2-RFP was coexpressed, over a sevenfold increase in the amount of Arf6wt bound to GGA1GAT-GST was observed (Figure 5). This augmentation is comparable to that induced by expression of specific Arf6 GEFs and indicates that MCOLN2 is an efficient Arf6 activator. The ability of MCOLN2 to promote activation of Arf6 is not a general characteristic of all the members of the mucolipin family, as MCOLN1 failed to increase the amount of Arf6 pulled down by the GGA1GAT protein (Figure S3A). We also carried out pull-down experiments with the constitutive active Arf6 (Arf6Q67L). As expected, Arf6Q67L bound GGA1GAT more efficiently than Arf6wt, but the amount of Arf6Q67L pulled down did not change after overexpression of MCOLN2, thus confirming that MCOLN2 promotes Arf6 activation (Figure S3B). Finally, we found that MCOLN2 did not activate Arf1, indicating that the observed effect is specific for Arf6 (Figure S3C).

MCOLN2 regulates recycling of internalized CD59 to the cell surface

Next we addressed the effect of overexpressing a MCOLN2 mutant on the trafficking of proteins through the Arf6-associated pathway. Members of the mucolipin family contain six transmembrane domains with the predicted ion pore located between transmembrane segments 5 and 6 (amino acids 496–521 for MCOLN1). It has recently been described for MCOLN1 that mutation of two aspartate residues located at the pore region to lysines (471DD/KK) affects ion selectivity and produces a inactive mutant that

cannot rescue transport of LacCer from lysosomes to Golgi in MLIV patient cells (26). Sequence alignment of the three mucolipin family members revealed a high degree of homology in the pore region and conservation of the two aspartate residues that are predicted to regulate ion specificity (Figure 6A). Based on this protein alignment, we generated a MCOLN2 mutant in which both D463 and D464 were mutated to lysines (MCOLN2-GFP-D^{463}D/KK).

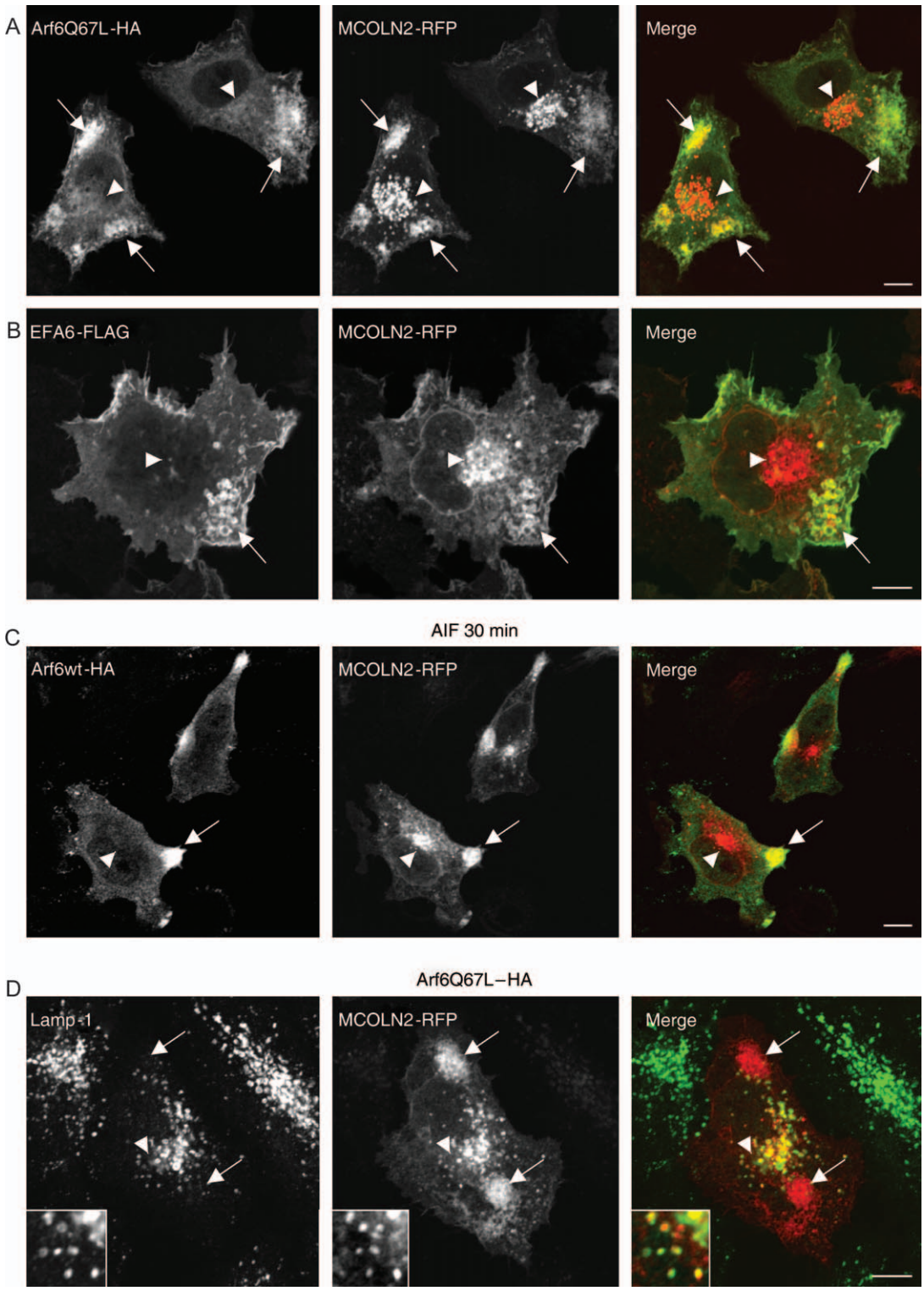

Figure 3: Legend on next page.

To assess the effect of MCOLN2-GFP-D^{463}D/KK mutant overexpression on the Arf6-associated pathway we measured traffic of CD59 by fluorescence-activated cell sorter (FACS) analysis. As, on average, less than a 30% of the cells were transfected with the MCOLN2-GFP-D^{463}D/KK mutant, the use of FACS allowed us to monitor CD59 traffic exclusively in cells overexpressing the mutant. In our assays, we incubated the cells with antibodies to CD59 at 37°C to label both plasma membrane and internal pools. After that the cells were (i) fixed and incubated with a secondary antibody to measure amount of CD59 at the plasma membrane or (ii) washed with acidic buffer to remove surface-bound CD59 antibodies, permeabilized, and incubated with secondary antibody to detect internalized CD59. As shown in Figure 6B,C, expression of MCOLN2-GFP-D^{463}D/KK did not significantly affect either the amount of CD59 at the plasma membrane or CD59 internalization when compared with control cells expressing GFP alone. We then address whether expression of MCOLN2-GFP-D^{463}D/KK could have an effect on the recycling of internalized CD59 to the plasma membrane, a process that is known to be regulated by Arf6 (16). Cells were incubated with antibodies to CD59 at 37°C for 30 min, washed with acidic buffer, and incubated at 37°C for 15 additional minutes to allow reappearance of internalized CD59 at the cell surface. Interestingly, in cells expressing MCOLN2-GFP-D^{463}D/KK the recycling of CD59 was considerably less efficient than in control cells (1.8-fold more recycled CD59 after 15 min in control cells versus MCOLN2-GFP-D^{463}D/KK expressing cells; $n = 9$) (Figure 6D). These data suggest that MCOLN2 may regulate recycling of internalized CD59 to the plasma membrane.

Finally, we depleted endogenous MCOLN2 by transfection of HeLa cells with specific siRNAs and examined the effect of this depletion on CD59 recycling. Because antibodies that recognize endogenous MCOLN2 are not available, we had to test the efficiency of our siRNA by transfecting MCOLN2-depleted cells with a plasmid that expresses recombinant MCOLN2. Previous reports have validated the use of such heterologously expressed fusion proteins for testing the efficiency of siRNAs (27). As seen in Figure S4A, transfection with a siRNA against MCOLN2 caused close to 90% reduction in the expression of recombinant MCOLN2-GFP without significantly affecting the levels of recombinant MCOLN1-GFP, MCOLN3-GFP, or Lamp-1-GFP, thus indicating that our siRNA mediates specific and efficient depletion of MCOLN2. Next we addressed whether depletion of MCOLN2 had an effect on CD59 recycling. Figure S4B shows that depletion of MCOLN2 caused close to a 20% reduction in the amount of internalized CD59 recycling back to the plasma membrane when compared with cells transfected with a control siRNA. Therefore our results indicate a role for MCOLN2 in the trafficking of cargo to the cell surface via the Arf6-regulated recycling pathway.

Discussion

The results presented in this paper indicate that MCOLN2 traffics through the Arf6-associated pathway. Two lines of evidence support this conclusion. First, when expressed in HeLa cells, MCOLN2-RFP colocalizes with MHCI and CD59 in long recycling endosomes; and second, expression of the Arf6Q67L mutant, which is defective in GTP hydrolysis, leads to the accumulation of MCOLN2-RFP into large vacuoles that also contain MHCI, CD59, and Arf6Q67L. Interestingly, overexpression of MCOLN2-RFP induces a strong activation of Arf6 *in vivo* as revealed by immunofluorescence and pull-down experiments. Therefore, MCOLN2 not only traffics through the Arf6 pathway, but might also regulate sorting of proteins that use this route. In agreement with this idea we found that overexpression of a MCOLN2 mutant that carries mutations predicted to affect pore selectivity (MCOLN2-GFP-D^{463}D/KK) dramatically decreased recycling of internalized CD59 to the cell surface. It has been shown that members of the mucolipin family have the ability to form homomultimers [(28) and our unpublished observations]. We predict that overexpression of MCOLN2-GFP-D^{463}D/KK causes sequestration of endogenous MCOLN2 into inactive channels, thus behaving as a dominant-negative mutant. The inhibitory effect of this dominant-negative mutant on the delivery of CD59 to the plasma membrane suggests that MCOLN2 plays an important role in the regulation of GPI-APs trafficking. We have also observed a delay in the recycling of CD59 to the cell surface after depletion of endogenous MCOLN2 by specific siRNAs. Although very reproducible, the delay in CD59 recycling caused by MCOLN2 depletion was not as strong as the one observed after MCOLN2-GFP-D^{463}D/KK overexpression. It is possible that incompleted depletion of endogenous MCOLN2 or functional redundancy with other members of the mucolipin family prevent us from obtaining a more drastic effect on CD59 trafficking.

Figure 3: Activation of endogenous Arf6 or overexpression of the Arf6Q67L mutant causes accumulation of MCOLN2-RFP in enlarged vacuoles. Hela cells were transfected with MCOLN2-RFP and either Arf6Q67L-HA (A and D), or EFA6-FLAG (B). Cells were fixed, permeabilized, and incubated with mouse antibody to HA (A), mouse antibody to FLAG (B) or rabbit antibody to Lamp-1 (D). Bound antibodies were revealed by staining with Alexa-488-conjugated antibodies. (C) HeLa cells were transfected with MCOLN2-RFP and Arf6wt-HA, and 15 h after transfection cells were treated with AlF for 30 min, fixed, permeabilized, and immunostained with mouse antibody to HA followed by Alexa-488-conjugated antibody to mouse IgG. Stained cells were examined by confocal fluorescence microscopy. Arrows indicate accumulation of MCOLN2-RFP in activate Arf6-positive vacuoles. Arrowheads denote the fraction of MCOLN2-RFP located at late endosomes—lysosomes, which is not affected by Arf6 activation. Insets in panel D show twofold magnifications of vesicles containing Lamp-1 and MCOLN2-RFP. Scale bar represents 10 μm.

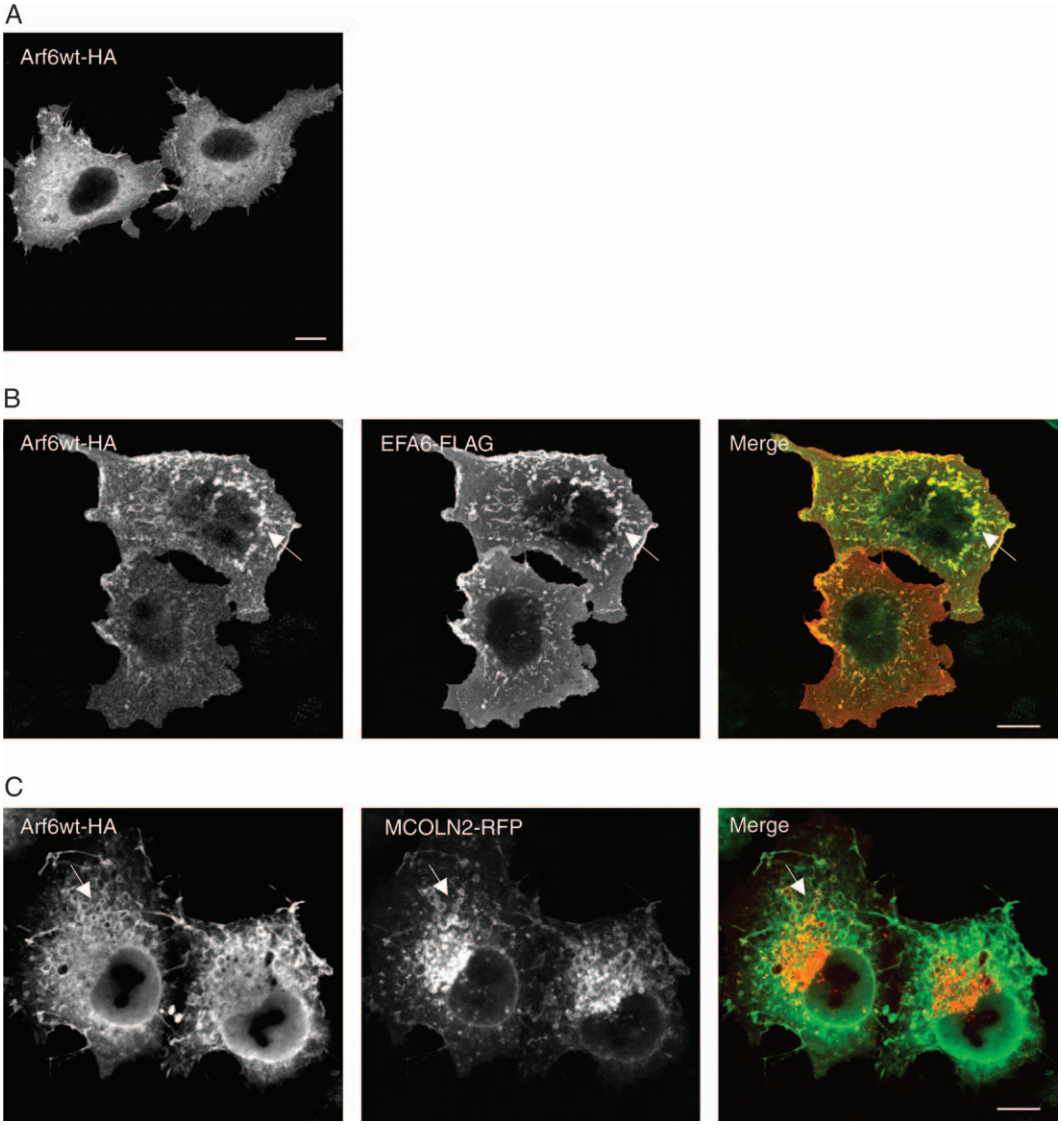

Figure 4: Overexpression of MCOLN2-RFP induces formation of Arf6-positive vacuoles. HeLa cells were transiently transfected with Arf6wt-HA alone (A) or cotransfected with constructs encoding Arf6wt-HA and EFA6-FLAG (B) or Arf6wt-HA and MCOLN2-RFP (C). Cells were fixed, permeabilized and incubated with monoclonal antibody to HA (A and C) or monoclonal antibody to FLAG and polyclonal antibody to HA (B). Bound antibodies were revealed by Alexa-488-conjugated antibody to mouse IgG (A and C) or by Alexa-555-conjugated antibody to mouse IgG and Alexa-488-conjugated antibody to rabbit IgG (B). All images were obtained by confocal microscopy. Arrows in B and C denote colocalization at enlarged vacuoles. Scale bar represents 10 μm.

In addition to the Arf6 pathway, a fraction of MCOLN2 was found in lysosomes. Accumulation of MCOLN2-RFP in Rab5Q79L-positive endosomes suggests that the protein travels through early endosomes before reaching lysosomes. Our results are consistent with the recent report of Venkatachalam et al. (28) that showed that mouse MCOLN2 tagged to HA or YFP is mostly localized at lysosomes and Rab11 positive vesicles in HEK293 cells. It will be of great interest to address whether MCOLN2 also has a role in the regulation of lysosomal function.

Trafficking of GPI-APs may vary slightly in different cell types. In Chinese hamster ovary (CHO) cells, GPI-APs are internalized from the plasma membrane through tubular invaginations and delivered to a GPI-anchored protein-enriched early endosomal compartment (GEECs) (29). From GEECs, GPI-APs reach recycling endosomes and are recycled back to the plasma membrane. In contrast, in baby hamster kidney (BHK) cells, GPI-APs traffic from the surface to EEA1-positive early endosomes and are subsequently delivered to late endosomes (30). Finally, in HeLa cells, recycling of GPI-APs is known to be dependent of Arf6 activity (16,31). Recently, it has been proposed that specific endocytic routes followed by GPI-APs in different cell types may correlate with the strength of association of GPI-APs with lipid rafts (30). Thus, in BHK cells, GPI-APs

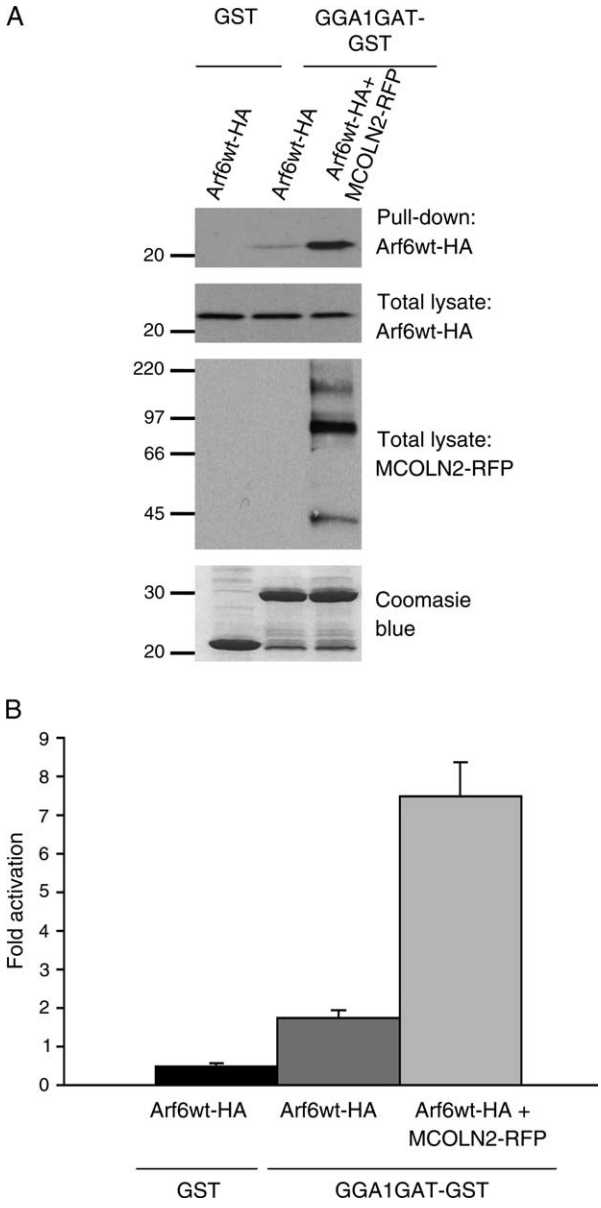

Figure 5: MCOLN2-RFP induces Arf6 activation. A) HeLa cells were transfected with either Arf6wt-HA alone or together with MCOLN2-RFP for 24 h, and pull-down assays were carried out using GST or GGA1GAT-GST to isolate GTP-bound Arf6. Immunoblot of the pull-downs and the total lysates was performed using antibodies to HA-tag and RFP. A Coomassie blue staining was carried out from pull-downs. B) Quantification of GTP-bound Arf6. Data shown are mean standard deviation of at least four independent experiments.

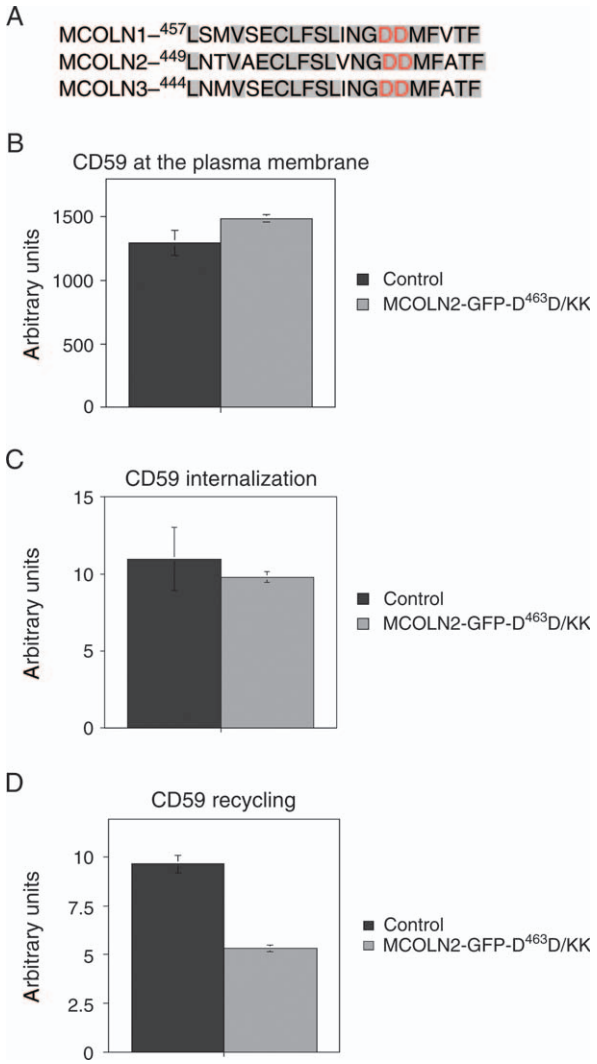

Figure 6: Overexpression of an inactive MCOLN2 mutant decreases the rate of CD59 recycling to the plasma membrane. A) Alignment of part of the pore region of the human mucolipin family. The two aspartate residues predicted to regulate ion selectivity are indicated in red. Residues conserved in the three human mucolipins are shared in gray. B–D) Effect of MCOLN2-GFP-D^{463}D/KK overexpression on CD59 traffic. HeLa cells were transfected with GFP alone (control) or with a MCOLN2 chimera that carries punctual mutations in the pore region (MCOLN2-GFP-D^{463}D/KK). After 15 h the cells were incubated at 37°C with monoclonal antibodies to CD59 and the total amount of CD59 at the plasma membrane (B), internalized (C), or recycled back to the cell surface (D) in transfected cells was quantified by FACS analysis as described in *Materials and Methods*.

remain associated with lipid rafts for long periods of time and this promotes transport to late endosomes. Conversely, in CHO cells, the time of residence of GPI-APs in lipid microdomains is considerably shorter, allowing GPI-APs to be delivered to recycling endosomes.

The location of MCOLN2 to tubular recycling endosomes together with its ability to activate Arf6 suggest that MCOLN2 may regulate trafficking between recycling endosomes and cell surface. Accordingly, our results showed that MCOLN2-GFP-D^{463}D/KK did not affect the amount of CD59 inside the cell after 5 min of internalization. However, we cannot discard that overexpression of this mutant causes retention of CD59 in an endosomal compartment or delivery to lysosomes, thus reducing the total CD59 recycled back to the plasma membrane.

How does MCOLN2 regulate trafficking of GPI-APs? One possibility is that MCOLN2 establishes lateral associations with some GPI-APs or GPI-AP receptors. Examples of lateral association of GPI-APs with transmembrane proteins are the interaction of CD14 with Toll-like receptor 4 (TLR4) to initiate LPS-mediated inflammatory response (32), or the association of the urokinase-type plasminogen activator receptor (uPAR) with β_1 and β_2 integrins in the regulation of cell migration (33). However, we have not detected any association of MCOLN2 with lipid rafts (our unpublished observations) suggesting that it is improbable that MCOLN2 directly interacts with GPI-APs. A second possibility is that MCOLN2 controls GPI-AP trafficking by regulating Arf6 activity. We have shown that MCOLN2 overexpression causes over a sevenfold increase in the amount of activated Arf6. The effect of MCOLN2 on Arf6 activity could be mediated by a direct interaction between both proteins. Alternatively, MCOLN2 could promote ARF6 activation by modulating the activity of specific Arf6 GEFs or GAPs. Understanding how MCOLN2 controls ARF6 activity will help to clarify the function of this protein. Finally, MCOLN2 could regulate the pH of an intracellular compartment where the sorting of GPI-APs takes place. It has been suggested that MCOLN1 may function primarily as a proton channel that modulates lysosomal acidification (34). MCOLN2 could also function as a proton channel and regulate pH in some endocytic compartment. Interestingly, GEECs from CHO cells are more acidic (pH $\approx$ 6.0) than sorting endosomes (pH $\approx$ 6.5), indicating that an effective acidification mechanism must be present (29). In addition, many proteins, including some GPI-APs such as the human prion protein PrP, are known to overcome pH-dependent oligomerization (35), and oligomerization seems to stabilize GPI-APs association with rafts (36). Therefore it is tempting to speculate that by regulating acidification, MCOLN2 could modulate the time of residence of GPI-APs into lipid rafts and, consequently, its intracellular trafficking (30). The two last hypotheses are not mutually exclusive. It has been shown that V-ATPase, a main regulator of endosomal acidification, binds Arf6 and ARNO in a pH-dependent manner, and that this interaction regulates trafficking of proteins in the degradative pathway (37). MCOLN2 could also regulate activation or recruitment of Arf6 to specific membranes depending on intravesicular acidification. Finally, it is important to note that a role for MCOLN1 in membrane fusion and fission events has also been suggested (38). Therefore, we cannot discard that MCOLN2 participates in the formation or dynamic of recycling endosomes.

In recent years there has been a growing interest in the study of the mucolipin family. MCOLN1 is the best-characterized member of this group because mutations in this protein cause MLIV. Although the exact function of MCOLN1 has not been determined, several groups have suggested a role in different trafficking events, including fusion between late endosomes and lysosomes (38), maintenance of lysosomal pH (34), and lysosomal secretion (39). MCOLN3 is also thought to be implicated in transport of melanosomes as a result of the defect in pigmentation observed in the *varitint-waddler* mouse. Here we assign to MCOLN2 a role in the regulation of the Arf6-associated pathway and, more specifically, in the trafficking of GPI-APs. Therefore, all three members of the mucolipin family have revealed themselves as important regulators of specific intracellular trafficking events.

Finally, Arf6 has been implicated not only in the regulation of intracellular trafficking and endocytosis, but also in actin remodeling, cell migration and cancer cell invasion (31,40). Future experiments will help to determine whether defects in the regulatory role of MCOLN2 on the Arf6-associated pathway may be associated with human pathologies.

Materials and Methods

Antibodies and reagents

The following antibodies were used: mouse monoclonal anti-CD63 (H5C6; Pharmingen); mouse monoclonal anti-EEA1 (BD Transduction Laboratories); mouse monoclonal anti-FLAG (Sigma); rabbit polyclonal anti-DsRed (Clontech Laboratories); rabbit anti-GFP (MBL International, Woburn, MA, USA); mouse monoclonal anti-HA (Covance); mouse monoclonal anti-CD59 (Chemicon). Mouse monoclonal anti-MHCI was a gift from Dr Julie Donaldson (NHLBI, NIH, Bethesda, MD, USA). Rabbit anti-Lamp-1 antibody was provided by Dr John Mort (Shriner's Hospital, Montreal, Canada). Protease inhibitor cocktail and glutathione and protein G-sepharose beads were obtained from Amersham Biosciences. ON-TARGETplus SMATpool siRNAs against MCOLN2 were from Dharmacon (Lafayette).

Plasmids

The complete open-reading frame of human MCOLN2 was PCR amplified from a human placenta cDNA library using specific primers and cloned into the Hind III-Sall sites of the pDs-Red-Monomer-N1 and the pEGFP-N1 vectors (Clontech) to generate MCOLN2-RFP and MCOLN2-GFP, respectively. Mutations of residues in MCOLN2 sequence were introduced using the QuickChange Site-Directed Mutagenesis Kit as per manufacturer's instructions (Stratagene). Site-directed mutations were confirmed by subsequent DNA sequencing. The MCOLN1-GFP vector was previously described (Vergarajauregui and Puertollano, 2006). GGA1GAT-GST was made in Dr Juan Bonifacino's Lab (NHCHD, NIH, Bethesda, MD, USA). Rab5Q79L-GFP is from Dr Robert Lodge (Laval, Quebec, Canada). Lamp-1-GFP is from Dr Esteban Dell'Angelica (UCLA, Los Angeles, CA, USA). Arf6wt-HA, Arf6Q67L-HA, EFA6-FLAG, and Arf1wt-HA plasmids were a kind gift from Dr Julie Donaldson (NHLBI, NIH, Bethesda, MD, USA).

Transfection and immunofluorescence microscopy

Transfection of HeLa cells was performed using either FuGENE-6 (Roche Molecular Biochemicals) or Nucleofector™ (Amaxa Inc.). For immunofluorescence, transfected HeLa cells were grown on coverslips, fixed in 4% paraformaldehyde for 15 min at room temperature and subsequently permeabilized in PBS, 0.2% (w/v) saponin for 10 min at room temperature. Incubation with primary antibodies diluted in PBS, 0.1% (w/v) saponin, 0.1% BSA was carried out for 1 h at room temperature. Unbound antibodies were removed by rinsing with PBS for 5 min, and cells were subsequently incubated with a secondary antibody diluted in PBS, 0.1% (w/v) saponin, 0.1% BSA, for 30–60 min at room temperature. After a final rinse with PBS, coverslips were mounted onto glass slides with Fluoromount G (Southern Biotechnology Associates, Birmingham, AL, USA). Fluorescence images were acquired on an LSM 510 confocal microscope (Carl Zeiss).

Pull-down experiments

HeLa cells were transfected with ARF6wt-HA alone or ARF6wt-HA plus MCOLN2-RFP using Nucleofector™, and 24 h later the cells were lysed in

0.2% Triton, 25 mM Tris–HCl pH 7.4, 150 mM NaCl, 5 mM ethylenediaminetetraacetic acid, and protease inhibitors. Lysates were precleared by centrifugation for 3 min at 16000g and then incubated with 80 μg of GGA1GAT-GST or GST bound to glutathione–sepharose beads overnight at 4°C. The beads were washed three times in PBS and eluted with SDS–PAGE sample buffer. The presence of ARF6-GTP was detected by immunoblot using an anti-HA antibody. Immunoblots were quantified using either the NIH image 1.63f software or the Odyssey infrared image system (LI-COR Biosciences).

Measurement of CD59 internalization and recycling by FACS

HeLa cells were transfected with a plasmid encoding GFP alone (control) or a MCOLN2 mutant (MCOLN2-GFP-D^{463}D/KK). Eighteen hours after transfection cells were harvested in Cellstripper™ solution (Mediatech, Inc.), washed once with PBS, placed in a water bath at 37°C, and incubated with 5 μL of monoclonal antibody to CD59 for 5 min. Unbound antibody was rinsed, and the cells were either fixed (4% paraformaldehyde v/v in PBS) to measure the amount of CD59 at the cell surface, or washed with acidic buffer (acetic acid 0.5%, NaCl 0.5 M) for 1 minute, fixed, and permeabilized (saponin 0.2% in PBS) to detect internalized CD59. Cells were then stained with a phycoerythrin-conjugated goat anti-mouse secondary antibody (dilution 1:100) for 30 min on ice, washed, and analyzed by flow cytometry using a FACS-Calibur and CellQuest software (BD Bioscience). To measure recycling of CD59, cells were incubated at 37°C with antibodies to CD59 for 30 min, washed with acidic buffer, placed at 37°C for 15 min to allow reappearance of internalized CD59 at the cell surface, fixed, incubated with secondary antibody, and analyzed by FACS. Amounts of protein were defined as the specific fluorescence value, which was calculated after subtracting background (fluorescence of cells incubated with secondary, but not primary antibody). Measurement of both phycoerythrin and GFP fluorescence allowed monitoring CD59 trafficking exclusively in transfected cells. Results were expressed as the mean ± standard deviation of at least three independent experiments.

Immunoblot

Immunoblotting was carried out according to standard procedures. Proteins were separated by SDS-PAGE and transferred to nitrocellulose. The membrane was then blocked with PBS/0.05% Tween-20/10% dry milk and incubated with the indicated antibodies. Enhanced chemiluminescence reagent (Amersham Bioscience) was used for detection.

Acknowledgments

We thank Julie Donaldson for helpful discussions and suggestions. We also appreciate the editorial assistance of the NIH Fellows Editorial Board. This project was supported by the Intramural Research Program of the NIH, National Heart, Lung, and Blood Institute (NHLBI).

Supplementary Materials

Figure S1: MCOLN2-RFP, CD59 and MHCI accumulate in ARF6Q67L-associated vacuolar endosomes. HeLa cells were transfected with plasmids encoding MCOLN2-RFP and ARFQ67L-HA. Fifteen hours after transfection the cells were fixed, permeabilized, and immunostained with antibodies to CD59 (A), MHCI and HA (B) or to CD59 and Lamp-1 (C). Arrows indicate ARF6Q67L-positive vacuoles. Arrowheads point to lysosomes. Inset in A shows a twofold magnification of the indicated region. Scale bar represents 10 μm.

Figure S2: MCOLN2 accumulates at Rab5Q79L-positive endosomes. HeLa cells were transiently cotransfected with plasmids encoding MCOLN2-RFP and Rab5Q79L. Fifteen hours after transfection cells were fixed and examined by confocal microscopy (A), or incubated with monoclonal antibodies against CD59 (B) or CD63 (C). Arrows indicate accumulation of MCOLN2-RFP in RabQ69L-positive vacuoles. Insets show twofold magnifications of the indicated regions. Scale bar represents 10 μm.

Figure S3: Specificity of MCOLN2-induced activation of Arf6. HeLa cells were transfected with: A) Arf6wt-HA alone or together with MCOLN1-RFP or MCOLN2-RFP; B) Arf6Q67L-HA alone or together with MCOLN2-RFP; C) Arf1-HA alone or together with MCOLN2-RFP for 24 h. Pull-down assays were carried out using GST or GGA1GAT-GST to isolate GTP-bound Arf6. Quantifications were performed from immunoblots using the Odyssey Infrared System.

Figure S4: Effect of MCOLN2 depletion on CD59 trafficking. A) HeLa cells expressing control siRNA or specific siRNA against MCOLN2 were transfected with Lamp-1-GFP, MCOLN1-GFP, MCOLN2-GFP or MCOLN3-GFP, lysated and resolved by 4–20% SDS–PAGE. Immunoblot analysis with antibodies against GFP revealed a band of approximately 90 KDa that correspond to predicted molecular weights for the monomeric forms of full-length MCOLN1-GFP, MCOLN2-GFP, and MCOLN3-GFP fusion proteins (arrow). Asterisks correspond to putative proteolytic forms, while higher bands correspond to dimers and oligomers (arrow). B) HeLa cells were transfected with control or MCOLN2 siRNAs. After 72 h, cells were incubated at 37°C with monoclonal antibodies to CD59 for 30 min, washed with acidic buffer, placed at 37°C for 15 min to allow reappearance of internalized CD59 at the cell surface, fixed, incubated with secondary antibody, and analyzed by FACS. The graphic represents the average of three independent experiments with triplicates for each condition.

Supplemental materials are available as part of the online article at http://www.blackwell-synergy.com

References

1. Pedersen SF, Owsianik G, Nilius B. TRP channels: an overview. Cell Calcium 2005;38:233–252.
2. Bach G, Cohen MM, Kohn G. Abnormal ganglioside accumulation in cultured fibroblasts from patients with mucolipidosis IV. Biochem Biophys Res Commun 1975;66:1483–1490.
3. Tellez-Nagel I, Rapin I, Iwamoto T, Johnson AA, Norton WT, Nitowsky H. Mucolipidosis IV: clinical, ultrastructural, histochemical and chemical studies of a case, including a brain biopsy. Arch Neurol 1976;33: 828–835.
4. Bach G, Zeigler M, Kohn G, Cohen MM. Mucopolysaccharides accumulation in cultured skin fibroblasts derived from patients with Mucolipidosis IV. Am J Hum Genet 1977;29:610–618.
5. Crandall BF, Philippart M, Brown WJ, Bluestone DA. Review article: mucolipidosis IV. Am J Med Genet 1982;12:301–308.
6. Fares H, Greenwald I. Regulation of endocytosis by CUP-5, the Caenorhabditis elegans mucolipin 1 homology. Nat Genet 2001;28:64–68.
7. Hersh BM, Hartwieg E, Horvitz RH. The Caenorhabditis elegans mucolipin-like gene CUP-5 is essential for viability and regulates lysosomes in multiple cell types. Proc Natl Acad Sci U S A 2002;99: 4355–4360.
8. Treusch S, Knuth S, Slaugenhaupt SA, Goldin E, Grant BD, Fares H. Caenorhabditis elegans functional orthologue of human protein h-mucolipin-1 is required for lysosome biogenesis. Proc Natl Acad Sci U S A 2004;101:4483–4488.
9. Di Palma F, Belyantseva IA, Kim HJ, Vogt TF, Kachar B, Noben-Trauth K. Mutations in Mcoln3 associated with deafness and pigmentation defects in varitint-waddler (Va) mice. Proc Natl Acad Sci U S A 2002; 99:14994–14999.

10. Lindvall JM, Blomberg KE, Wennborg A, Smith CI. Differential expression and molecular characterisation of Lmo7, Myo1e, Sash1, and Mcoln2 genes in Btk-defective B-cells. Cell Immunol 2005;235:46–55.
11. Vergarajauregui S, Puertollano R. Two di-leucine motifs regulate trafficking of mucolipin-1 to lysosomes. Traffic 2006;7:337–353.
12. Miedel MT, Weixel KM, Bruns JR, Traub LM, Weisz OA. Posttranslational cleavage and adaptor protein complex-dependent trafficking of mucolipin-1. J Biol Chem 2006;281:12751–12759.
13. Bonifacino JS, Traub LM. Signals for sorting of transmembrane proteins to endosomes and lysosomes. Annu Rev Biochem 2003;72:395–447.
14. Radhakrishna H, Donaldson JG. ADP-ribosylation factor 6 regulates a novel plasma membrane recycling pathway. J Cell Biol 1997;139: 49–61.
15. Brown FD, Rozelle AL, Yin HL, Balla T, Donaldson JG. Phosphatidylinositol 4,5-bisphosphate and Arf6-regulated membrane traffic. J Cell Biol 2001;154:1007–1017.
16. Naslavsky N, Weigert R, Donaldson JG. Characterization of a nonclathrin endocytic pathway: membrane cargo and lipid requirements. Mol Biol Cell 2004;15:3542–3552.
17. Weigert R, Yeung AC, Li J, Donaldson JG. Rab22a regulates the recycling of membrane proteins internalized independently of clathrin. Mol Biol Cell 2004;15:3758–3770.
18. Caplan S, Naslavsky N, Hartnell LM, Lodge R, Polishchuk RS, Donaldson JG, Bonifacino JS. A tubular EHD1-containing compartment involved in the recycling of major histocompatibility complex class I molecules to the plasma membrane. EMBO J 2002;21:2557–2567.
19. Jovanovic OA, Brown FD, Donaldson JG. An effector domain mutant of Arf6 implicates phospholipase D in endosomal membrane recycling. Mol Biol Cell 2006;17:327–335.
20. Martinu L, Masuda-Robens JM, Robertson SE, Santy LC, Casanova JE, Chou MM. The TBC (Tre-2/Bub2/Cdc16) domain protein TRE17 regulates plasma membrane- endosomal trafficking through activation of Arf6. Mol Cell Biol 2004;24:9752–9762.
21. Naslavsky N, Weigert R, Donaldson JG. Convergence of non-clathrin- and clathrin-derived endosomes involves Arf6 inactivation and changes in phosphoinositides. Mol Biol Cell 2003;14:417–431.
22. Franco M, Peters PJ, Boretto J, van Donselaar E, Neri A, D'Souza-Schorey C, Chavrier P. EFA6, a sec7 domain-containing exchange factor for ARF6, coordinates membrane recycling and actin cytoskeleton organization. EMBO J 1999;18:1480–1491.
23. Santy LC, Casanova JE. Activation of ARF6 by ARNO stimulates epithelial cell migration through downstream activation of both Rac1 and phospholipase D. J Cell Biol 2001;154:599–610.
24. Niedergang F, Colucci-Guyon E, Dubois T, Raposo G, Chavrier P. ADP ribosylation factor 6 is activated and controls membrane delivery during phagocytosis in macrophages. J Cell Biol 2003;161:1143–1150.
25. Macia E, Luton F, Partisani M, Cherfils J, Chardin P, Franco M. The GDP-bound form of Arf6 is located at the plasma membrane. J Cell Sci 2004;117:2389–2398.
26. Pryor PR, Reimann F, Gribble FM, Luzio JP. Mucolipin-1 is a lysosomal membrane protein required for intracellular lactosylceramide traffic. Traffic 2006;7:1388–1398.
27. Huang F, Khvorova A, Marshall W, Sorkin A. Analysis of clathrin-mediated endocytosis of epidermal growth factor receptor by RNA interference. J Biol Chem 2004;279:16657–16661.
28. Venkatachalam K, Hofmann T, Montell C. Lysosomal localization of TRPML3 depends on TRPML2 and the mucolipidosis-associated protein TRPML1. J Biol Chem 2006;281:17517–17527.
29. Kalia M, Kumari S, Chadda R, Hill MM, Parton RG, Mayor S. Arf6-independent GPI-anchored protein-enriched early endosomal compartments fuse with sorting endosomes via a Rab5/phosphatidylinositol-3'-kinase-dependent machinery. Mol Biol Cell 2006;17:3689–3704.
30. Fivaz M, Vilbois F, Thurnheer S, Pasquali C, Abrami L, Bickel PE, Parton RG, van der Goot FG. Differential sorting and fate of endocytosed GPI-anchored proteins. EMBO J 2002;21:3989–4000.
31. Donaldson JG. Multiple roles for Arf 6, sorting, structuring and signaling at the plasma membrane. J Biol Chem 2003;278:41573–41576.
32. Miller SI, Ernst RK, Bader MW. LPS, TLR4 and infectious disease diversity. Nat Rev Microbiol 2005;3:36–46.
33. Ragno P. The urokinase receptor: a ligand or a receptor? Story of a sociable molecule. Cell Mol Life Sci 2006;63:1028–1037.
34. Soyombo AA, Tjon-Kon-Sang S, Rbaibi Y, Bashllari E, Bisceglia J, Muallem S, Kiselyov K. TRP-ML1 regulates lysosomal pH and acidic lysosomal lipid hydrolytic activity. J Biol Chem 2006;281:7294–7301.
35. Zahn R. The octapeptide repeats in mammalian prion protein constitute a pH-dependent folding and aggregation site. J Mol Biol 2003;334: 477–488.
36. Paladino S, Sarnataro D, Pillich R, Tivodar S, Nitsch L, Zurzolo C. Protein oligomerization modulates raft partitioning and apical sorting of GPI-anchored proteins. J Cell Biol 2004;167:699–709.
37. Hurtado-Lorenzo A, Skinner M, El Annan J, Futai M, Sun-Wada GH, Bourgoin S, Casanova J, Wildeman A, Bechoua S, Ausiello DA, Brown D, Marshansky V. V-ATPase interacts with ARNO and Arf6 in early endosomes and regulates the protein degradative pathway. Nat Cell Biol 2006;8:124–136.
38. Piper RC, Luzio JP. CUPpling calcium to lysosomal biogenesis. Trends Cell Biol 2004;14:471–473.
39. Laplante JM, Sun M, Falardeau J, Dai D, Brown EM, Slaugenhaupt SA, Vassilev PM. Lysosomal exocytosis is impaired in mucolipidosis type IV. Mol Genet Metab 2006;89:339–348.
40. D'Souza-Schorey C, Chavrier P. ARF proteins: roles in membrane traffic and beyond. Nat Rev Mol Cell Biol 2006;7:347–358.